How strong the electron-phonon interaction in metals can be?

Emil Yuzbashyan

RUTGERS
THE STATE UNIVERSITY
OF NEW JERSEY

EY & **Boris Altshuler**, Migdal-Eliashberg theory as a classical spin chain, Phys. Rev. B (2022)

EY & **Boris Altshuler**, Breakdown of the Migdal-Eliashberg theory…, Phys. Rev. B (2022)

Special thanks to **Dmitrii Semenok**
Center for High Pressure Science & Technology Advanced Research, Beijing, China

AIP Conference Proceedings **4**, 17 (1972)

COMMENTS ON THE MAXIMUM SUPERCONDUCTING TRANSITION TEMPERATURE

Marvin L. Cohen*
University of California, Berkeley, Cal. 94720

P.W. Anderson+
Cavendish Laboratory, Cambridge, England
Bell Laboratories, Murray Hill, New Jersey, 07974

ABSTRACT

Using current superconductivity theory and some assumptions about the normal state properties of solids, estimates of the maximum superconducting transition temperature are made. The optimum resonant frequency for an attractive interaction, the role of umklapp scattering, and the appearance of lattice instabilities are discussed.

PHYSICAL REVIEW VOLUME 108, NUMBER 5 DECEMBER 1, 1957

Theory of Superconductivity*

J. BARDEEN, L. N. COOPER,† AND J. R. SCHRIEFFER‡
Department of Physics, University of Illinois, Urbana, Illinois
(Received July 8, 1957)

- Effective low-energy theory valid in the weak coupling limit only

$$\hat{H}_{\mathrm{BCS}} = \sum_{\boldsymbol{k},\sigma} \epsilon_{\boldsymbol{k}} \hat{c}^{\dagger}_{\boldsymbol{k}\sigma} \hat{c}_{\boldsymbol{k}\sigma} - \frac{\lambda}{N_0} \sum_{\substack{|\epsilon_{\boldsymbol{k}}|<\Omega \\ |\epsilon_{\boldsymbol{p}}|<\Omega}} \hat{c}^{\dagger}_{\boldsymbol{k}\uparrow} \hat{c}^{\dagger}_{-\boldsymbol{k}\downarrow} \hat{c}_{-\boldsymbol{p}\downarrow} \hat{c}_{\boldsymbol{p}\uparrow}$$

- Attraction between electrons of opposite momenta in an energy window $(-\Omega, \Omega)$ centered on the Fermi level

- Ω – ultraviolet cutoff of the order of the typical phonon energy, e.g., the Debye energy. “This cutoff corresponds to forming our wave function from states in the region where the interaction is expected to be attractive and not mixing in states outside this region.”

- Emerges from the high-energy (Eliashberg) theory in the weak coupling limit $\lambda \to 0$

BCS Theory

$$1 = \lambda \int_0^{\Omega} \frac{d\epsilon}{\sqrt{\epsilon^2 + \Delta^2}} \tanh \frac{\sqrt{\epsilon^2 + \Delta^2}}{2T}$$

Self-consistency equation

const

const

$$\Delta(T = 0) = \Omega \exp\left(-\frac{1}{\lambda}\right)$$

$$T_c = \Omega \exp\left(-\frac{1}{\lambda}\right)$$

$$T_c \approx 0.57\Delta(T = 0)$$

?

$$\lambda = \left[\ln\left(\frac{T_c}{\Omega}\right)\right]^{-1}$$

$\lambda = ?$ $\Omega = ?$

What if $\lambda > 1$?

Isotope effect

$\Downarrow$

Electron-Phonon Interaction

?

Electron-phonon Hamiltonians

Holstein Hamiltonian

$$H = \sum_{\boldsymbol{ij}\sigma} t_{\boldsymbol{ij}} c^\dagger_{\boldsymbol{i}\sigma} c_{\boldsymbol{j}\sigma} + \sum_{\boldsymbol{i}} \left[\frac{p_{\boldsymbol{i}}^2}{2M} + \frac{K_0 x_{\boldsymbol{i}}^2}{2} \right] + \alpha \sum_{\boldsymbol{i}} n_{\boldsymbol{i}} x_{\boldsymbol{i}}$$

T. Holstein, Studies of polaron motion…, Ann. Phys. **8**, 325 (1959)

A. Einstein, Planck’s theory of radiation and the theory of the specific heat, Ann. d. Physik **22**, 180 (1907)

Einstein in 1905

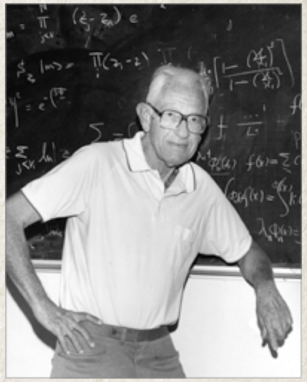

Theodore Holstein

Fröhlich Hamiltonian

$$H = \sum_{\boldsymbol{p}\sigma} \xi_{\boldsymbol{p}} c^\dagger_{\boldsymbol{p}\sigma} c_{\boldsymbol{p}\sigma} + \sum_{\boldsymbol{q}} \omega_0(\boldsymbol{q}) b^\dagger_{\boldsymbol{q}} b_{\boldsymbol{q}} + \sum_{\boldsymbol{pq}\sigma} g_{\boldsymbol{q}} c^\dagger_{\boldsymbol{p}+\boldsymbol{q}\sigma} c_{\boldsymbol{p}\sigma} \left[b^\dagger_{-\boldsymbol{q}} + b_{\boldsymbol{q}} \right]$$

H. Frölich, Electrons in lattice fields, Adv. Phys. **3**, 325 (1954)

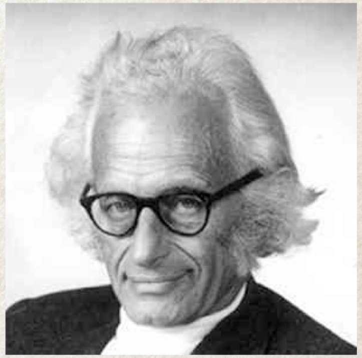

Herbert Fröhlich

Main conclusions are independent of the choice of the effective Hamiltonian, so let us work with the Holstein Hamiltonian

$$H = \underbrace{\sum_{\boldsymbol{ij}\sigma} t_{\boldsymbol{ij}} c^\dagger_{\boldsymbol{i}\sigma} c_{\boldsymbol{j}\sigma}}_{\text{Electron hopping}} + \underbrace{\sum_{\boldsymbol{i}} \left[\frac{p_{\boldsymbol{i}}^2}{2M} + \frac{K_0 x_{\boldsymbol{i}}^2}{2} \right]}_{\text{Lattice oscillators}} + \underbrace{\alpha \sum_{\boldsymbol{i}} n_{\boldsymbol{i}} x_{\boldsymbol{i}}}_{\text{Electron-phonon interaction}}$$

$n_{\boldsymbol{i}}$ – number of electrons on site $\boldsymbol{i}$

INTERACTION BETWEEN ELECTRONS AND LATTICE VIBRATIONS IN A NORMAL METAL

J. Exptl. Theoret. Phys. (U.S.S.R.) **34**, 1438-1446 (June, 1958)

A method is developed which enables one to obtain the electron-energy spectrum and dispersion of the lattice vibrations without assuming that the interaction between electrons and phonons is small.

A. B. Migdal

INTERACTIONS BETWEEN ELECTRONS AND LATTICE VIBRATIONS IN A SUPERCONDUCTOR

J. Exptl. Theoret. Phys. (U.S.S.R.) **38**, 966-976 (March, 1960)

A perturbation theory is developed for the Green's function in which the Green's function calculated for the superconducting ground state is used as the zero approximation. Dyson equations are written down from which the electron Green's function can be determined. Interaction between electrons and phonons is not assumed to be small. The spectrum and the damping of the excitations are calculated.

G. M. Eliashberg

Phonon-mediated electron-electron interaction

$$U(\omega) = \frac{g^2}{\omega^2 + \Omega^2}, \qquad \Omega^2 = \frac{K}{M}, \quad g^2 = \frac{\nu_0 \alpha^2}{M}$$

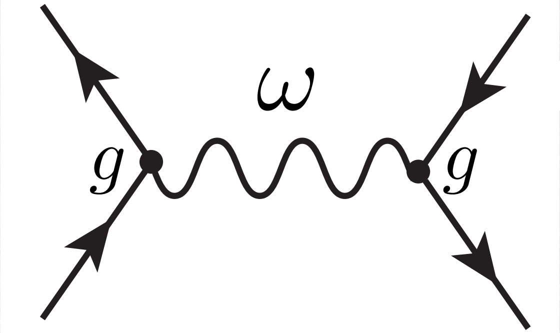

Electrons renormalize (modify) lattice vibrations

K – renormalized spring const of lattice oscillators

Main parameter: dimensionless electron-phonon coupling const: $\lambda = \frac{g^2}{\Omega^2} = \frac{\nu_0 \alpha^2}{K}$

Weak coupling limit (BCS theory)

Phonon-mediated electron-electron interaction: $U(\omega) = \dfrac{g^2}{\omega^2 + \Omega^2}$ $\qquad \lambda \equiv \dfrac{g^2}{\Omega^2}$

At $\lambda \ll 1$ frequencies relevant for superconductivity $\omega \sim \Delta(T=0) = \Omega e^{-1/\lambda} \ll \Omega$

$$\Longrightarrow \quad U(\omega) \approx \lambda \quad \Longrightarrow \quad U(\tau - \tau') = \lambda \delta(\tau - \tau')$$

Instantaneous interaction (non-retarded)

$$\Longrightarrow \quad \hat{H}_{\text{int}} = -\frac{\lambda}{N_0} \sum_{\boldsymbol{p}\boldsymbol{p}'\boldsymbol{q}} c^\dagger_{\boldsymbol{p}+\boldsymbol{q}\uparrow} c^\dagger_{\boldsymbol{p}'-\boldsymbol{q}\downarrow} c_{\boldsymbol{p}'\downarrow} c_{\boldsymbol{p}\uparrow}$$

$$\Longrightarrow \quad \hat{H} = \hat{H}_{\text{BCS}} = \sum_{\boldsymbol{k},\sigma} \epsilon_{\boldsymbol{k}} \hat{c}^\dagger_{\boldsymbol{k}\sigma} \hat{c}_{\boldsymbol{k}\sigma} - \frac{\lambda}{N_0} \sum_{\substack{|\epsilon_{\boldsymbol{k}}|<\Omega \\ |\epsilon_{\boldsymbol{p}}|<\Omega}} \hat{c}^\dagger_{\boldsymbol{k}\uparrow} \hat{c}^\dagger_{-\boldsymbol{k}\downarrow} \hat{c}_{-\boldsymbol{p}\downarrow} \hat{c}_{\boldsymbol{p}\uparrow}$$

Path integral formulation of the Migdal-Eliashberg theory

$$L(\tau) = \sum_{\boldsymbol{ij},\sigma} c^*_{\boldsymbol{i}\sigma} G^{-1}_{\boldsymbol{ij}} c_{\boldsymbol{j}\sigma} + \sum_{\boldsymbol{i}} \left[\frac{K x_{\boldsymbol{i}}^2}{2} + \frac{M(\partial_\tau x_{\boldsymbol{i}})^2}{2} \right] + \alpha \sum_{\boldsymbol{i}\sigma} c^*_{\boldsymbol{i}\sigma} c_{\boldsymbol{i}\sigma} x_{\boldsymbol{i}}, \qquad S = \int_0^\beta d\tau L(\tau)$$

$$G^{-1}_{\boldsymbol{ij}} = \partial_\tau \delta_{\boldsymbol{ij}} + t_{\boldsymbol{ij}} - \mu \delta_{\boldsymbol{ij}}$$

1. Integrate out phonons
2. Decouple e-e interactions with Hubbard-Stratonovich fields $\Sigma_\uparrow(\tau', \tau)$, $\Sigma_\downarrow(\tau', \tau)$, $\Phi(\tau', \tau)$
3. Integrate out electrons to obtain an effective action in terms of the Hubbard-Stratonovich fields only
4. Stationary point of the effective action = Migdal-Eliashberg theory

Fluctuations around the stationary point negligible in the limit: $E_F \to \infty$

Stationary point equations = Eliashberg equations:

$$\Phi_n = \pi T \sum_m U_{nm} \frac{\Phi_m}{\sqrt{(\omega_m + \Sigma_m)^2 + |\Phi_m|^2}}, \quad \Sigma_n = \pi T \sum_m U_{nm} \frac{\omega_m + \Sigma_m}{\sqrt{(\omega_m + \Sigma_m)^2 + |\Phi_m|^2}}$$

$$U_{nm} = U(\omega_n - \omega_m)$$

$\omega_n = \pi T(2n+1)$ – fermionic Matsubara frequency

$\Sigma_n \equiv \Sigma(\omega_n), \;\; \Phi_n \equiv \Phi(\omega_n)$ – normal & anomalous self-energies

Σ_n is real

Φ_n is complex

Stationary point equations = Eliashberg equations:

$$\Phi_n = \pi T \sum_m U_{nm} \frac{\Phi_m}{\sqrt{(\omega_m + \Sigma_m)^2 + |\Phi_m|^2}}, \quad \Sigma_n = \pi T \sum_m U_{nm} \frac{\omega_m + \Sigma_m}{\sqrt{(\omega_m + \Sigma_m)^2 + |\Phi_m|^2}}$$

$U_{nm} = U(\omega_n - \omega_m)$ $\Sigma_n \equiv \Sigma(\omega_n), \;\; \Phi_n \equiv \Phi(\omega_n)$ – normal & anomalous self-energies

$\omega_n = \pi T(2n+1)$ – fermionic Matsubara frequency

Introduce Green's functions: $\Phi(\tau) = \pi U(\tau) F(\tau), \quad \Sigma(\tau) = \pi U(\tau) G(\tau)$
(energy-integrated)

Stationary point eqs $\Longrightarrow F_n = \dfrac{\Phi_n}{\sqrt{(\omega_n + \Sigma_n)^2 + |\Phi_n|^2}}, \quad G_n = \dfrac{\omega_n + \Sigma_n}{\sqrt{(\omega_n + \Sigma_n)^2 + |\Phi_n|^2}}$

Stationary point constraint: $G_n^2 + |F_n|^2 = 1$

Stationary point constraint: $G_n^2 + |F_n|^2 = 1 \quad \Longrightarrow \quad \boldsymbol{S}_n^2 = 1$

Components of a classical spin $\boldsymbol{S}_n$ of unit length: $S_n^z = G_n, \quad S_n^x = \mathrm{Re}(F_n), \quad S_n^y = \mathrm{Im}(F_n)$

Can rewrite the effective action (free energy functional) in terms of spins, i.e., map the Migdal-Eliashberg theory to a classical spin chain!

Free energy density:

$$f = \nu_0 T^2 \sum_{nl} \left[\Phi^*_{n+l} U_l^{-1} \Phi_n + \Sigma_{n+l} U_l^{-1} \Sigma_n\right] - 2\pi\nu_0 T \sum_n \sqrt{(\omega_n + \Sigma_n)^2 + |\Phi_n|^2}$$

In terms of the classical spins $\boldsymbol{S}_n$ it becomes a spin chain Hamiltonian:

$$H_s = -2\pi \sum_n \omega_n S_n^z - \pi^2 T g^2 \sum_{nm} \frac{\boldsymbol{S}_n \cdot \boldsymbol{S}_m - 1}{(\omega_n - \omega_m)^2 + \Omega^2}$$

Solutions of Eliashberg equations = Spin equilibria

Free energy minimum = Spin chain ground state

$$f = \nu_0 T H_s$$

Migdal-Eliashberg theory in terms of classical spins

$$H_s = -2\pi \sum_n \omega_n S_n^z - \pi^2 T g^2 \sum_{nm} \frac{\boldsymbol{S}_n \cdot \boldsymbol{S}_m - 1}{(\omega_n - \omega_m)^2 + \Omega^2}$$

Sites of the chain – fermionic Matsubara frequencies $\omega_n = \pi T(2n+1)$

Ferromagnetic Heisenberg model in inhomogeneous Zeeman field

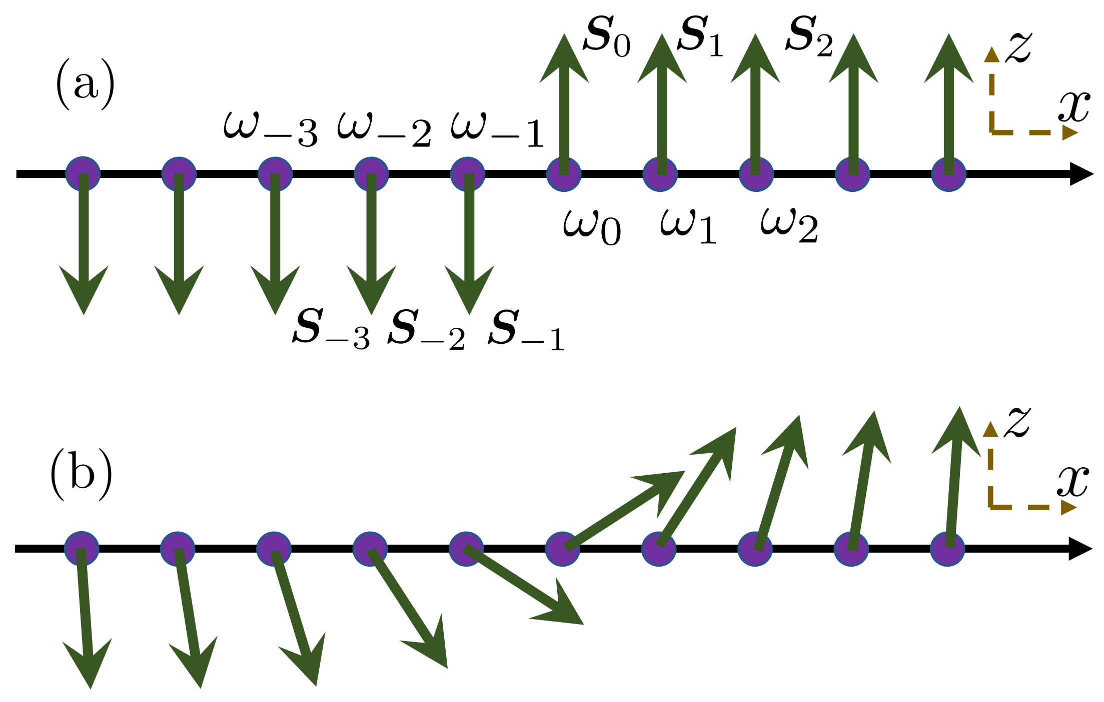

$$S_n^z = G_n, \quad S_n^x = \mathrm{Re}(F_n), \quad S_n^y = \mathrm{Im}(F_n)$$

a) Normal state: all spins parallel to the z axis

$$F_n = 0 \qquad \boldsymbol{S}_n = \mathrm{sgn}(\omega_n)\hat{\boldsymbol{z}}$$

a) Superconducting state: spins acquire x components. Superconducting transition: softening of the domain wall at the origin

$$F_n \neq 0$$

Migdal-Eliashberg theory in terms of classical spins

$$H_s = -2\pi \sum_n \omega_n S_n^z - \pi^2 T g^2 \sum_{nm} \frac{\boldsymbol{S}_n \cdot \boldsymbol{S}_m - 1}{(\omega_n - \omega_m)^2 + \Omega^2}$$

Sites of the chain – fermionic Matsubara frequencies $\omega_n = \pi T(2n+1)$

Ferromagnetic Heisenberg model in inhomogeneous Zeeman field

Spin-chain representation makes previously unknown properties easy to see.

Example: new ("spin-flip") solutions of the Eliashberg equations (probably play a role in kinetics)

Recall: Solutions of Eliashberg equations = Spin equilibria

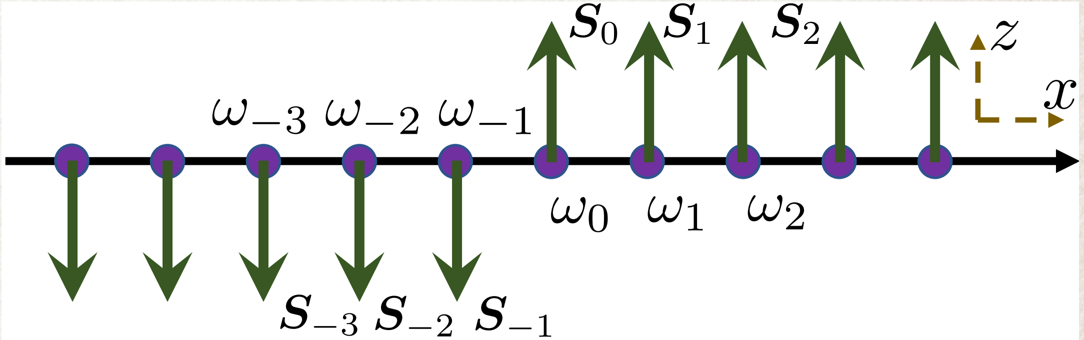

EY and Altshuler (2022)

Migdal-Eliashberg theory in terms of classical spins

$$H_s = -2\pi \sum_n \omega_n S_n^z - \pi^2 T g^2 \sum_{nm} \frac{\boldsymbol{S}_n \cdot \boldsymbol{S}_m - 1}{(\omega_n - \omega_m)^2 + \Omega^2}$$

Sites of the chain – fermionic Matsubara frequencies $\omega_n = \pi T(2n+1)$

Ferromagnetic Heisenberg model in inhomogeneous Zeeman field

Spin-chain representation makes previously unknown properties easy to see.

Example: new (“spin-flip”) solutions of the Eliashberg equations (probably play a role in kinetics)

Recall: Solutions of Eliashberg equations = Spin equilibria

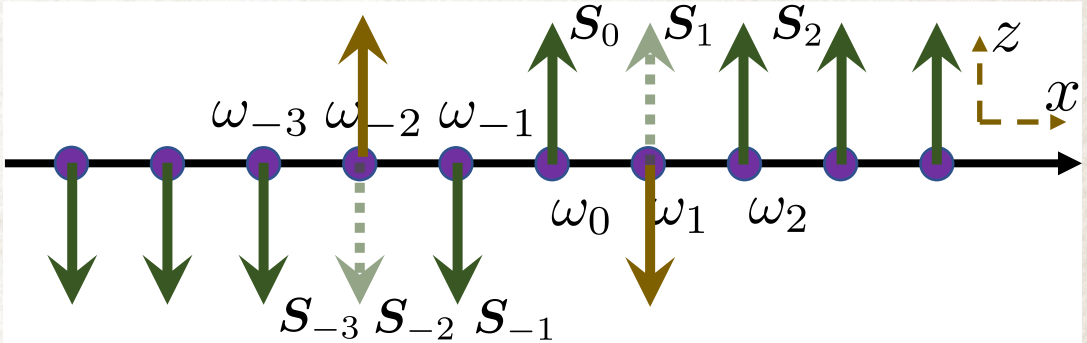

EY and Altshuler (2022)

Universality of the strong coupling limit $\lambda \to \infty$

$$\lambda = \frac{g^2}{\Omega^2} = \frac{\nu_0 \alpha^2}{K} \to \infty$$ equivalent to $\Omega \to 0$ or $K \to 0$ (free ion limit)

$$\Omega^2 = \frac{K}{M}, \qquad g^2 = \frac{\nu_0 \alpha^2}{M}$$

Universality of the strong coupling limit $\lambda \to \infty$

$$\lambda = \frac{g^2}{\Omega^2} = \frac{\nu_0 \alpha^2}{K} \to \infty$$ equivalent to $\Omega \to 0$ or $K \to 0$ (free ion limit)

$$H_s = -2\pi \sum_n \omega_n S_n^z - \pi^2 T \sum_{nm} U_{nm} \left(\boldsymbol{S}_n \cdot \boldsymbol{S}_m - 1 \right) \qquad U_{nm} = \frac{g^2}{(\omega_n - \omega_m)^2 + \Omega^2}$$

Dispersing phonons: $U_{nm} = \frac{1}{2p_F^2} \int_0^{2p_F} \frac{g_q^2 q dq}{(\omega_n - \omega_m)^2 + \omega_q^2}$

In all cases $U_{nm} \to \frac{g^2}{(\omega_n - \omega_m)^2}$ in the strong coupling limit

Universality of the strong coupling limit $\lambda \to \infty$

$$\lambda = \frac{g^2}{\Omega^2} = \frac{\nu_0 \alpha^2}{K} \to \infty$$ equivalent to $\Omega \to 0$ or $K \to 0$ (free ion limit)

In all cases $U_{nm} \to \dfrac{g^2}{(\omega_n - \omega_m)^2}$ in the strong coupling limit, i.e., this limit is universal (independent of microscopic details)

Single energy scale g. $T_c \approx 0.18g = 0.18\Omega\sqrt{\lambda} \to \infty$ T_c is unbounded

Any results we obtain at strong coupling are similarly universal. Note that the weak coupling limit of the ME theory (BCS theory) is also universal – governed by a single energy scale Δ_0

Bergmann & Rainer (1973), Allen & Dynes (1975), Carbotte (1990), Combescot (1995).

T_c in the strong coupling limit

$$T_c \approx 0.18g = 0.18\Omega\sqrt{\lambda} \to \infty$$

T_c is unbounded

Really?

Can T_c be arbitrarily large

Can λ be arbitrarily large

?

Normal state specific heat

Free energy: $f = \nu_0 T H_s = -2\pi\nu_0 T \sum_n \omega_n S_n^z - \pi^2 \nu_0 T^2 g^2 \sum_{nm} \frac{\boldsymbol{S}_n \cdot \boldsymbol{S}_m - 1}{(\omega_n - \omega_m)^2 + \Omega^2}$

Normal state: $\boldsymbol{S}_n = \mathrm{sgn}(\omega_n)\hat{\boldsymbol{z}}$

Electronic specific heat: $C_\mathrm{n} = -T\frac{d^2 f}{dT^2}$

Normal state specific heat

Free energy: $f = \nu_0 T H_s = -2\pi\nu_0 T \sum_n \omega_n S_n^z - \pi^2 \nu_0 T^2 g^2 \sum_{nm} \frac{\boldsymbol{S}_n \cdot \boldsymbol{S}_m - 1}{(\omega_n - \omega_m)^2 + \Omega^2}$

Normal state: $\boldsymbol{S}_n = \mathrm{sgn}(\omega_n)\hat{\boldsymbol{z}}$

Electronic specific heat: $C_\mathrm{n} = \gamma_0 T \left[1 + \lambda h \left(\frac{\Omega}{2\pi T} \right) \right]$

$$h(x) = -6x^2 - 12x^3 \mathbf{Im}[\psi'(ix)] - 6x^4 \mathbf{Re}[\psi''(ix)]$$

$\gamma_0 = \frac{2\pi^2 \nu_0}{3}, \quad \psi(x)$ – digamma function

Prange & Kadanoff (1964), Grimvall (1969), Lee & Rainer (1988), EY & Altshuler (2022)

Normal state specific heat

Electronic specific heat: $C_\mathrm{n} = \gamma_0 T \left[1 + \lambda h\left(\frac{\Omega}{2\pi T}\right)\right] \quad \gamma_0 = \frac{2\pi^2\nu_0}{3}, \quad \psi(x)$ – digamma function

$$h(x) = -6x^2 - 12x^3 \mathrm{Im}[\psi'(ix)] - 6x^4 \mathrm{Re}[\psi''(ix)]$$

$C_\mathrm{n} < 0$ for $\lambda > 3.69$ and $T_- < T < T_+$

$T_+ > T_c$ for all λ

$$T_c \approx 0.18\sqrt{\lambda}\Omega$$

$$T_+ \approx 0.38\sqrt{\lambda}\Omega$$

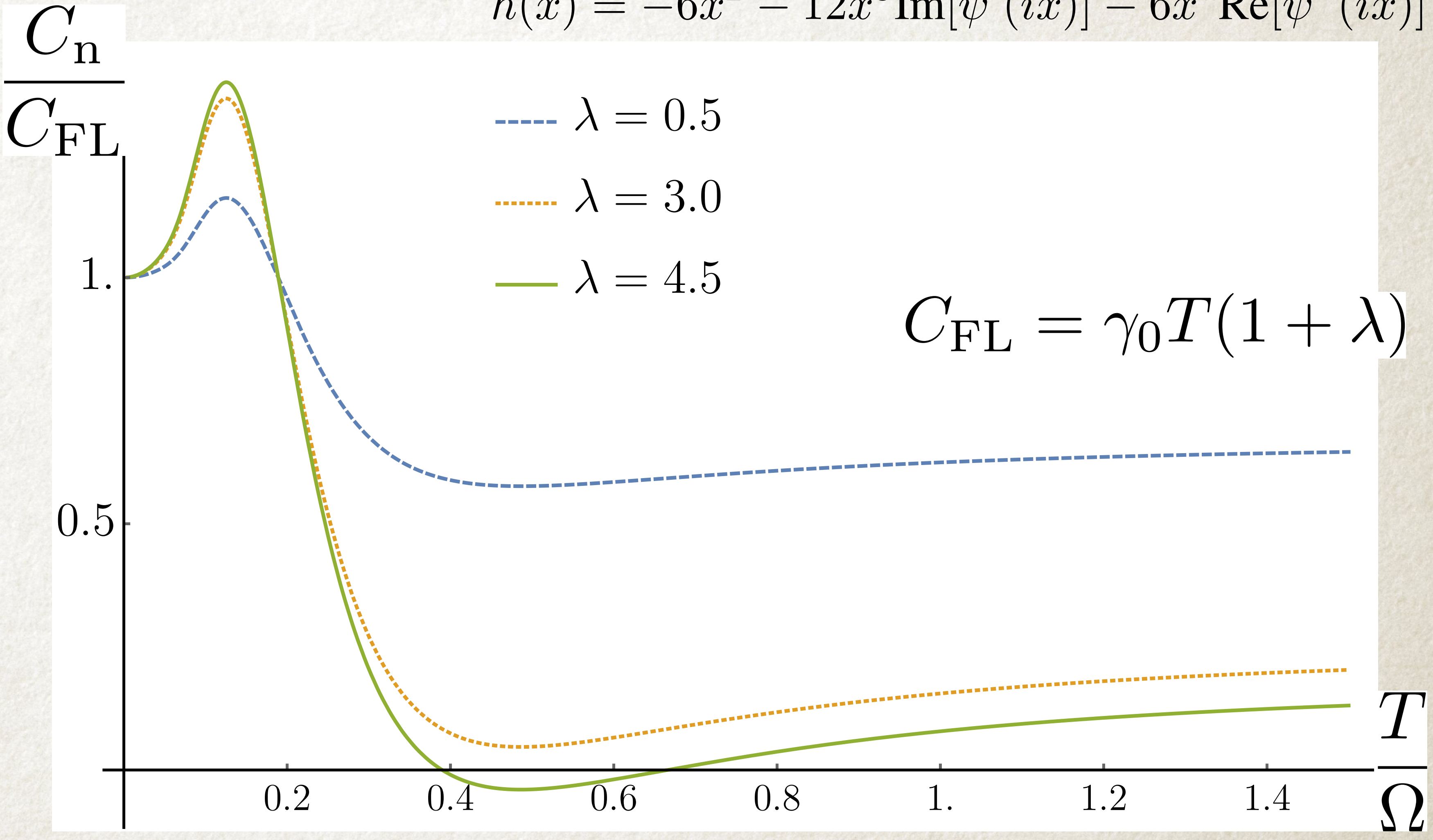

EY and Altshuler (2022)

Normal state specific heat

$C_\mathrm{n}(T) < 0$ for $\lambda > 3.7$ and $T_- < T < T_+$ $T_+ > T_c$ for all λ

The system is thermodynamically unstable!

Migdal-Eliashberg theory breaks down for $\lambda > \lambda_c \approx 3.69$

By construction, it is still a stationary point but no longer the global minimum.

Cannot have a metal with $\lambda \gtrsim 3.69$!

Since the strong coupling limit is universal, these conclusions are independent of the microscopic Hamiltonian, though λ_c can vary somewhat between models

EY and Altshuler (2022)

Material	λ	T_c/Ω
Al	0.43	0.004
V	0.80	0.031
Ta	0.69	0.035
Sn	0.72	0.038
Tl	0.80	0.046
$Tl_{0.9}Bi_{0.1}$	0.78	0.048
In	0.81	0.050
Nb (Butler)	1.22	0.057
Nb (Arnold)	1.01	0.062
$V_3Si_{-}1$	1.00	0.070
V_3Si (Kihl.)	1.00	0.071
Nb (Rowell)	0.98	0.074
Mo	0.90	0.076
$Pb_{0.4}Tl_{0.6}$	1.15	0.095
La	0.98	0.099
V_3Ga	1.14	0.103
Nb_3Al (2)	1.20	0.113
Nb_3Ge (2)	1.60	0.114
$Pb_{0.6}Tl_{0.4}$	1.38	0.119
Pb	1.55	0.128
Nb_3Al (3)	1.70	0.129
$Pb_{0.8}Tl_{0.2}$	1.53	0.136
Hg	1.62	0.146
Nb_3Sn	1.70	0.146
$Pb_{0.9}Bi_{0.1}$	1.66	0.152
Nb_3Al (1)	1.70	0.156
Nb_3Ge (1)	1.60	0.160
$Pb_{0.8}Bi_{0.2}$	1.88	0.172
$Pb_{0.7}Bi_{0.3}$	2.01	0.182
$Pb_{0.65}Bi_{0.35}$	2.13	0.200
$Pb_{0.5}Bi_{0.5}$	3.00	0.320
Ga	2.25	0.243
$Pb_{0.75}Bi_{0.25}$	2.76	0.288
Bi	2.45	0.320

Must have: $\lambda \lesssim 3.69$

$$T_c \approx 0.18\Omega\sqrt{\lambda}$$

$$\Downarrow$$

$$\frac{T_c}{\Omega} \lesssim 0.35$$

Experimental values for various metals

Carbotte, Rev. Mod. Phys (1990)

Table 1. Highest critical temperatures obtained experimentally and theoretically in the harmonic approximation (at $\mu^* = 0.1$) of some hydride superconductors. The theoretical T_C values presented have been obtained before the publication of experimental works. Because it is difficult to find data for the same pressure, the comparison is shown for illustration only.

Compound	Experimental pressure, GPa	Estimated T_C, K	Experimental T_C, K
$Im\bar{3}m$-H_3S	150	200 [15]	203 [5]
$Fm\bar{3}m$-LaH_{10}	160	286 [18, 19]	250-260 [7, 8]
$P6_3/mmc$-YH_9	200	303 [19, 103]	243 [31]
$Im\bar{3}m$-YH_6	170	270 [104]	224 [30]
$Fm\bar{3}m$-ThH_{10}	170	160–193 [27]	161 [27]
$P6_3/mmc$-UH_7	70	46 [26]	8 [47]
$F\bar{4}3m$-PrH_9	150	56 [36]	6 [25]
$P6_3/mmc$-CeH_9	110	117 [28, 29]	~90 [105]
$Fm\bar{3}m$-CeH_{10}	100	168 [106]	~115 [105]
c-SnH_x	190	81–97 [107]	76 [108]
PH_x	200	~100 [109]	100 [110]
$Pm\bar{3}n$-AlH_3	110	>24 [111, 112]	<4 [112, 113]
$Im\bar{3}m$-CaH_6	170	220–235 [114]	215 [115]

Must have: $\lambda \lesssim 3.69$ $T_c \approx 0.18\Omega\sqrt{\lambda}$

Ab initio values for lanthanum hydride, Errea et.al., Nature (2020)

System	Pressure (GPa)	λ	ω_{log} (meV)	$T_{c\,ani}^{ME}$ (K)
LaH_{10}	129	3.62	76.4	255.3
LaH_{10}	163	2.67	96.4	242.8
LaH_{10}	214	2.06	115.5	237.9
LaH_{10}	264	1.73	126.6	216.9
LaD_{10}	159	3.14	63.5	180.4
LaD_{10}	210	2.21	81.7	172.9
LaD_{10}	260	1.80	92.2	157.9

Notice that λ increases with decreasing pressure

Dmitrii Semenok
Private Communication

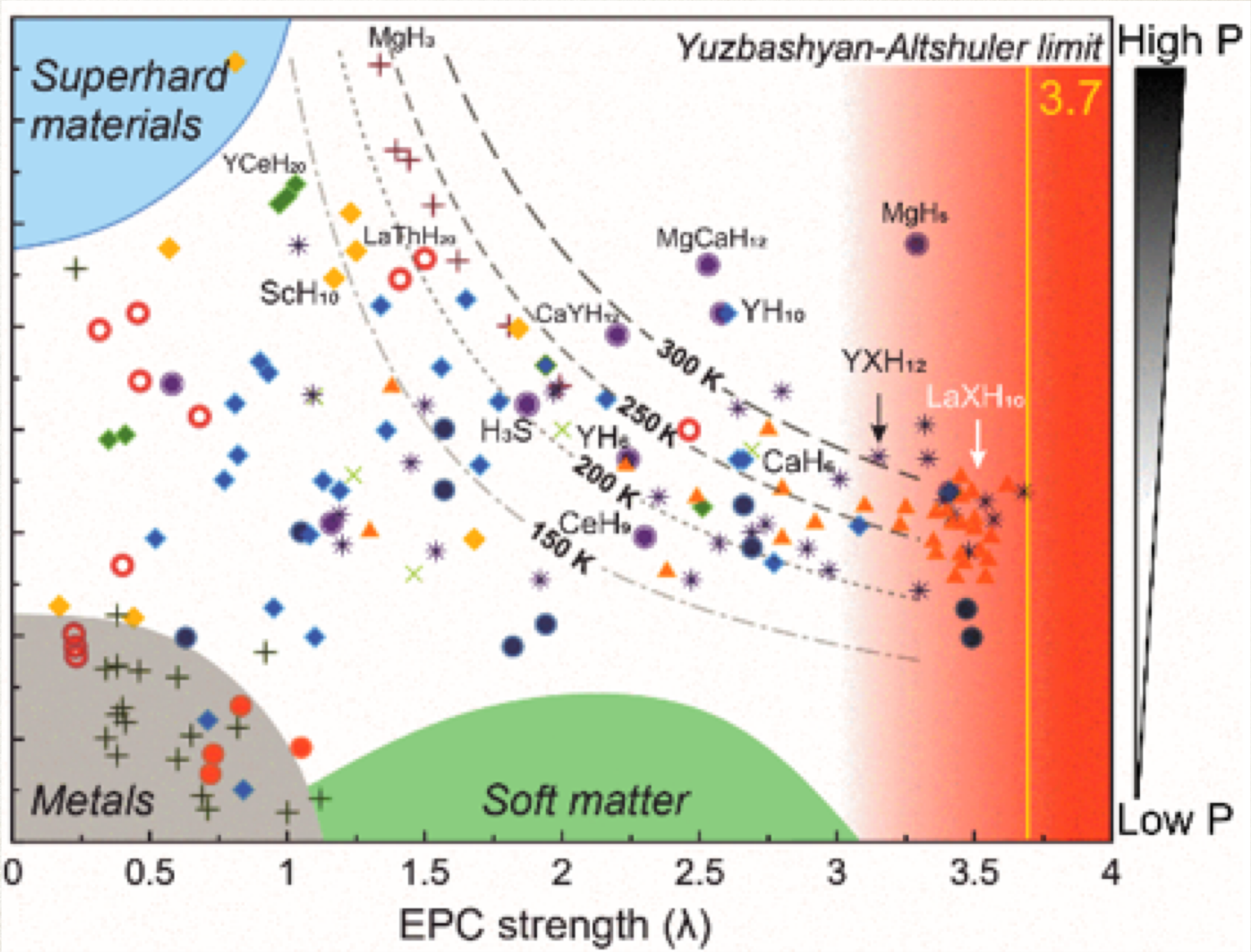

The source of instability at large λ

A gap at the Fermi level lowers the energy (and makes specific heat positive)

- ❖ Insulating or superconducting gap **?**
- ❖ Metastable Superconductivity **?**

1) $\lambda < \lambda_c \approx 3.7$ Normal state stable above T_c^{sc}. Metal-Superconductor transition

Free energy profile:

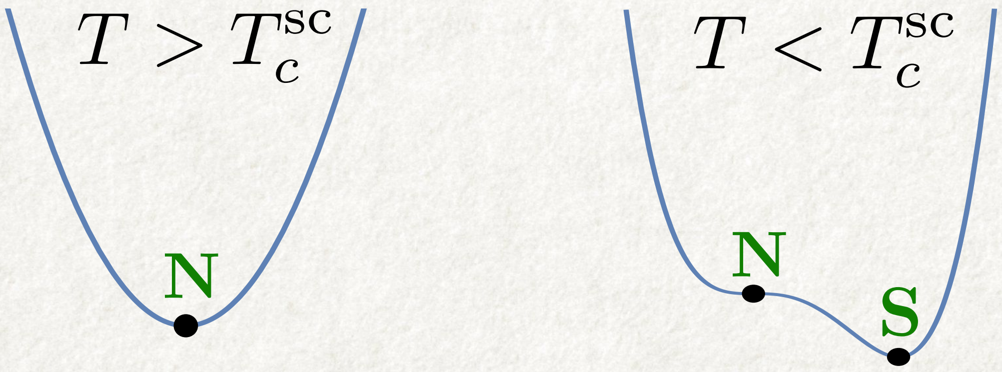

2) $\lambda > \lambda_c \approx 3.7$ Normal state unstable above T_c^{sc}. Metal-NS-Superconductor(?) transition.

$T_+ \approx 0.38\sqrt{\lambda}\Omega$

$T_c^{\mathrm{sc}} \approx 0.18\sqrt{\lambda}\Omega$

Free energy profile:

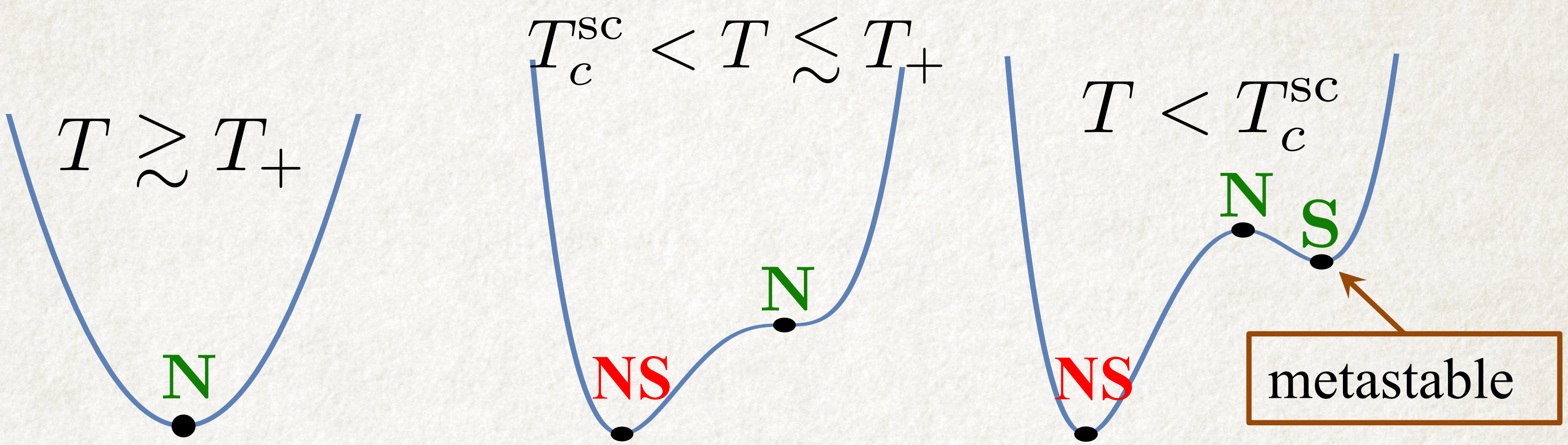

NS = (a) metal with smaller λ (due to a structural transition) or (b) insulator

At first, **NS** wins over **S**, i.e., **S** is metastable. At even lower T, **S** can win or **NS** can become superconducting, i.e., stable **S** but with lower T_c

2) $\lambda > \lambda_c \approx 3.7$ Normal state unstable above $T_c^{\rm sc}$. Metal-NS-Superconductor(?) transition.

$$T_+ \approx 0.38\sqrt{\lambda}\Omega$$

$$T_c^{\rm sc} \approx 0.18\sqrt{\lambda}\Omega$$

Free energy profile:

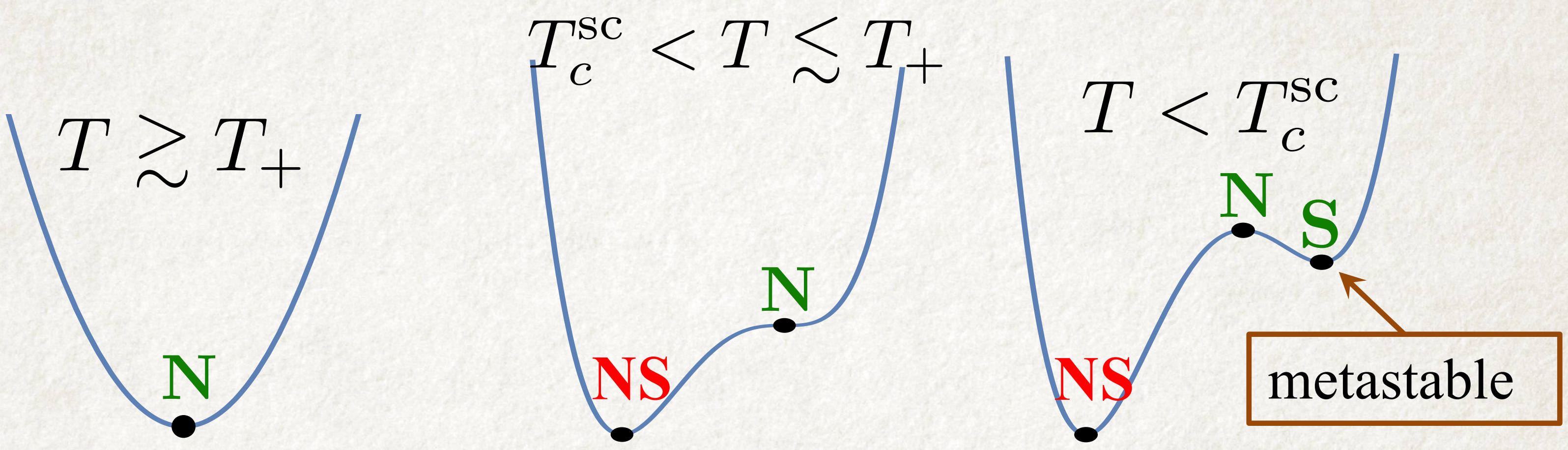

NS = (a) metal with smaller λ (due to a structural transition) or (b) insulator

At first, **NS** wins over **S**, i.e., **S** is metastable. At even lower T, **S** can win or **NS** can become superconducting, i.e., stable **S** but with lower T_c

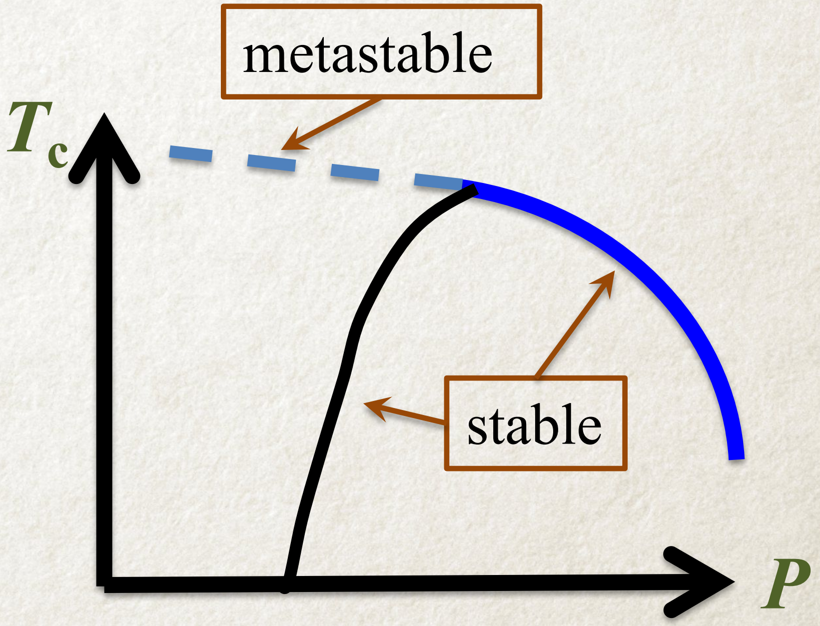

Pressure-induced high-temperature superconductivity retained without pressure in FeSe single crystals

Liangzi Deng[a,b,1], Trevor Bontke[a,b], Rabin Dahal[a,b], Yu Xie[c,d], Bin Gao[e], Xue Li[c,d], Ketao Yin[f], Melissa Gooch[a,b], Donald Rolston[a,b], Tong Chen[e], Zheng Wu[a,b], Yanming Ma[c,d], Pengcheng Dai[e], and Ching-Wu Chu[a,b,g,1]

PNAS 2021 Vol. 118 No. 28 e2108938118

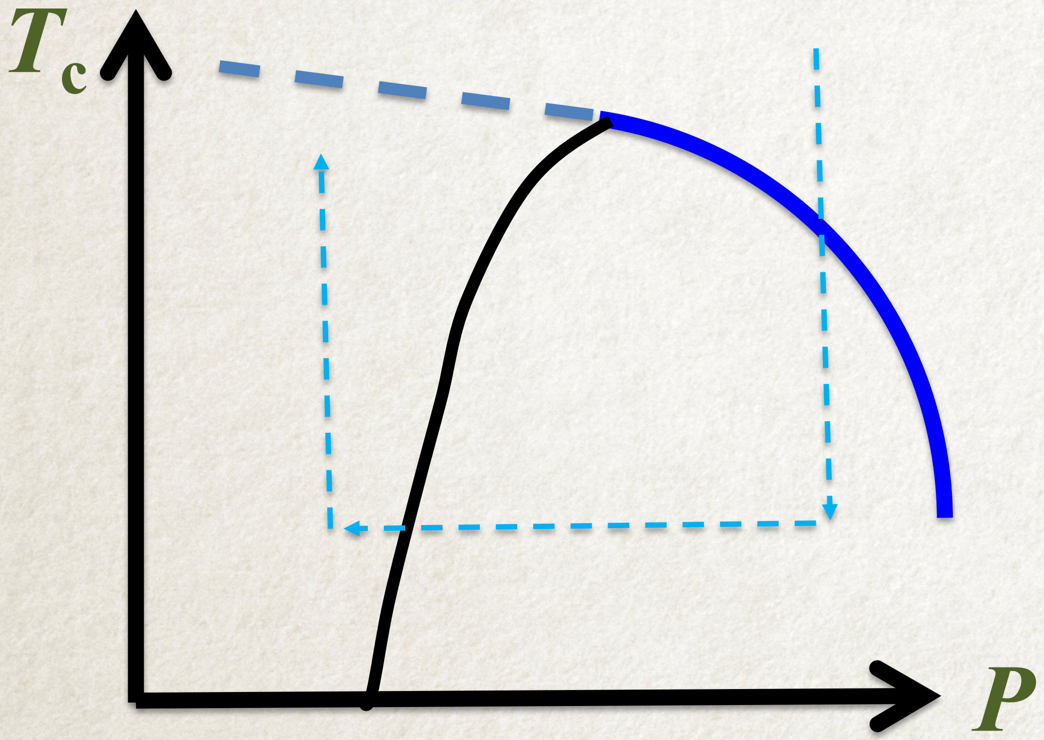

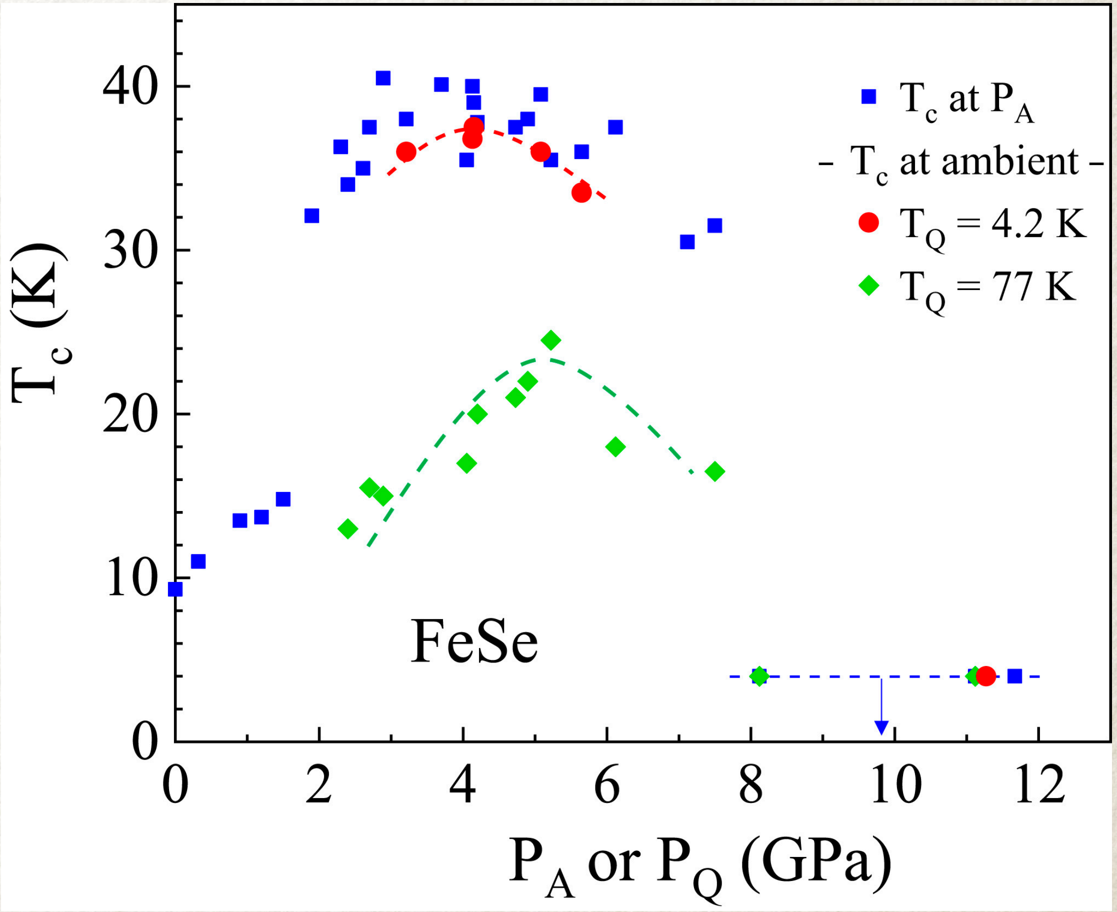

Quasiparticle lifetime τ at large λ

Normal state thermal Green's function: $\mathcal{G}_{\boldsymbol{p}}(\omega_n) = \dfrac{1}{i\omega_n + i\Sigma_n - \xi_{\boldsymbol{p}}}$

Recall: $\Sigma(\tau) = \pi U(\tau) G(\tau) \qquad G_n = S_n^z = \mathrm{sgn}(\omega_n)$

$$\Sigma_n = \pi T g^2 \sum_m \frac{G_n}{(\omega_n - \omega_m)^2 + \Omega^2} = \pi T g^2 \sum_m \frac{\mathrm{sgn}(\omega_n)}{(\omega_n - \omega_m)^2 + \Omega^2} \to \lambda \pi T \mathrm{sgn}(\omega_n)$$

Quasiparticle lifetime τ at large λ

Retarded Green's function: $G^R_{\boldsymbol{p}}(\omega) = \dfrac{1}{\omega - \xi_{\boldsymbol{p}} + i\lambda\pi T}$

Quasiparticle decay rate: $\Gamma = \tau^{-1} = \lambda\pi T$

Quasiparticle lifetime: $\tau \to 0$ as $\lambda \to \infty$

Fermionic quasiparticles are ill-defined

Qualitative picture of the breakdown

$$H_{\mathrm{el-ph}} = \alpha \sum_{\boldsymbol{i}} n_{\boldsymbol{i}} x_{\boldsymbol{i}}$$

At strong coupling $T \gg \Omega \Rightarrow$ phonons are classical

Qualitative picture of the breakdown

$$H_{\mathrm{el-ph}} = \alpha \sum_{\boldsymbol{i}} n_{\boldsymbol{i}} x_{\boldsymbol{i}} = \sum_{\boldsymbol{i}} V_{\boldsymbol{i}} n_{\boldsymbol{i}}$$

At strong coupling $T \gg \Omega \Rightarrow$ phonons are classical

Can interpret $V_{\boldsymbol{i}} = \alpha x_{\boldsymbol{i}}$ as a random (impurity) potential

Qualitative picture of the breakdown

$$H_{\rm el-ph} = \alpha \sum_{\boldsymbol{i}} n_{\boldsymbol{i}} x_{\boldsymbol{i}} = \sum_{\boldsymbol{i}} V_{\boldsymbol{i}} n_{\boldsymbol{i}}$$

At strong coupling $T \gg \Omega \Rightarrow$ phonons are classical

Can interpret $V_{\boldsymbol{i}} = \alpha x_{\boldsymbol{i}}$ as a random (impurity) potential

Decay rate due to nonmagnetic impurities: $\Gamma_{\rm imp} = \pi \nu_0 \langle V_{\boldsymbol{i}}^2 \rangle$ In our case: $\langle V_{\boldsymbol{i}}^2 \rangle = \alpha^2 \langle x_{\boldsymbol{i}}^2 \rangle$

By equipartition theorem for harmonic oscillator: $\dfrac{K \langle x_{\boldsymbol{i}}^2 \rangle}{2} = \dfrac{T}{2}$

Recall: $\lambda = \dfrac{\nu_0 \alpha^2}{K}$

We have: $\Gamma_{\rm imp} = \lambda \pi T$

EY and Altshuler (2022)

Qualitative picture of the breakdown

$$H_{\mathrm{el-ph}} = \alpha \sum_{\boldsymbol{i}} n_{\boldsymbol{i}} x_{\boldsymbol{i}} = \sum_{\boldsymbol{i}} V_{\boldsymbol{i}} n_{\boldsymbol{i}}$$

At strong coupling $T \gg \Omega \Rightarrow$ phonons are classical

Can interpret $V_{\boldsymbol{i}} = \alpha x_{\boldsymbol{i}}$ as a random (impurity) potential

Decay rate due to nonmagnetic impurities: $\Gamma_{\mathrm{imp}} = \pi \nu_0 \langle V_{\boldsymbol{i}}^2 \rangle$ In our case: $\langle V_{\boldsymbol{i}}^2 \rangle = \alpha^2 \langle x_{\boldsymbol{i}}^2 \rangle$

By equipartition theorem for harmonic oscillator: $\dfrac{K \langle x_{\boldsymbol{i}}^2 \rangle}{2} = \dfrac{T}{2}$

Recall: $\lambda = \dfrac{\nu_0 \alpha^2}{K}$

We have: $\Gamma_{\mathrm{imp}} = \lambda \pi T = \Gamma_{\mathrm{ME}}$

Vanishing of the quasiparticle lifetime is due to classical phonons: thermal fluctuations of static ion displacements

The role of classical phonons

$$H = \sum_{ij\sigma} t_{ij} c^\dagger_{i\sigma} c_{j\sigma} + \sum_i \left[\frac{\bar{p}_i^2}{2M} + \frac{K \bar{x}_i^2}{2} \right] + \alpha \sum_i n_i \bar{x}_i$$

Classical momenta integrate out (they are independent variables).

The role of classical phonons

$$H = \sum_{ij\sigma} t_{ij} c^{\dagger}_{i\sigma} c_{j\sigma} + \underbrace{\sum_{i} \frac{K \bar{x}_i^2}{2}}_{\text{elastic energy}} + \underbrace{\alpha \sum_{i} n_i \bar{x}_i}_{\text{potential}}$$

Classical momenta integrate out (they are independent variables).

We have electrons moving in a potential $V_i = \alpha \bar{x}_i$, which comes at an elastic energy cost. At strong coupling $K \to 0$ and the elastic energy cost disappears.

Indeed, recall that the strong coupling limit $\lambda = \frac{\nu_0 \alpha^2}{K} \to \infty$ is the free ion limit $K \to 0$

The role of classical phonons

$$H = \sum_{ij\sigma} t_{ij} c^\dagger_{i\sigma} c_{j\sigma} + \underbrace{\sum_i \frac{K\bar{x}_i^2}{2}}_{\text{elastic energy}} + \underbrace{\alpha \sum_i n_i \bar{x}_i}_{\text{potential}}$$

Classical momenta integrate out (they are independent variables).

We have electrons moving in a potential $V_i = \alpha \bar{x}_i$, which comes at an elastic energy cost. At strong coupling $K \to 0$ and the elastic energy cost disappears.

Indeed, recall that the strong coupling limit $\lambda = \frac{\nu_0 \alpha^2}{K} \to \infty$ is the free ion limit $K \to 0$

Inevitably, at some point it becomes energetically favorable to generate a nonuniform potential for electrons, i.e., $\bar{x}_i$ acquire nonzero averages. Lattice translational symmetry breaks and charge-density-wave (CDW) order develops.

EY and Altshuler (2022)

Peierls (CDW) instability: toy example

$$H = \sum_{\boldsymbol{ij}\sigma} t_{\boldsymbol{ij}} c^\dagger_{\boldsymbol{i}\sigma} c_{\boldsymbol{j}\sigma} + \sum_{\boldsymbol{i}} \frac{K\bar{x}_{\boldsymbol{i}}^2}{2} + \alpha \sum_{\boldsymbol{i}} n_{\boldsymbol{i}} \bar{x}_{\boldsymbol{i}}$$

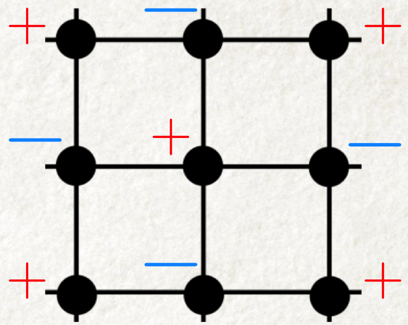

Square lattice, near half filling

(π,π) lattice distortion pattern: $\bar{x}_{\boldsymbol{i}} = X_{\text{c.m.}} + (-1)^{i_x+i_y}\delta x$

Quasiparticle spectrum: $E_{\boldsymbol{k}} = \pm\sqrt{\varepsilon_{\boldsymbol{k}}^2 + \Delta_P^2}$, $\Delta_P = \alpha\delta x$ – Peierls gap

The solution with $\delta x \neq 0$ has lower energy breaking the translational symmetry of the original lattice.

Gaps opens at the Fermi energy: Metal-insulator transition. At lower fillings can also be FL to FL transition accompanied by lattice translational symmetry breaking. Or structural transition at $\lambda \leq \lambda_c$ resulting in a lower value of λ